DOI 10.1007/s11041-020-00512-5
*Metal Science and Heat Treatment*, Vol. 62, Nos. 1 – 2, May, 2020 (Russian Original Nos. 1 – 2, January – February, 2020)

UDC 669-176:669.017.3

# STRUCTURAL AND TEXTURAL STATES OF STEEL 06G2MB STRIPS AFTER CONTROLLED THERMOMECHANICAL TREATMENT

**S. I. Platov,[1] M. L. Krasnov,[2] N. V. Urtsev,[3] S. V. Danilov,[4] and M. L. Lobanov[4]**

Translated from *Metallovedenie i Termicheskaya Obrabotka Metallov*, No. 1, pp. 56 – 61, January, 2020.

Orientation microscopy (EBSD) is used to study structural and textural states through the thickness of pipe steel strips after a controlled thermomechanical treatment. It is shown that texture formation in the form of a selection of components (3 – 7) with a large number of versions of crystallographic orientations, arising with shear phase transformations in accordance with the orientation ratios, suggests presence within the steel structure of elements limiting the number of possible α′-phase orientations. It is proposed that these elements are special boundaries formed during hot rolling close to boundaries RSU Σ3 and Σ11 between deformed austenite grains.

***Key words:*** pipe steels, thermomechanical controlled processing (TMCP), bainite, martensite, orientation microscopy, texture, orientation ratios, special boundaries.

## INTRODUCTION

Production of metal semiproducts and functional components as a rule is implemented in the form of directional deformation and heat treatment, and leads to formation within them of a volumetric (integral) texture. Presence of a texture gives objects a certain level of orientation-dependent physical and mechanical properties and control of them by occurrence and development makes it possible to optimize well-known and to develop new technology [1 – 4]. Formation of an integral material texture proceeds due to summation of the results of processes implemented at a sub-micron level: dislocation sliding during deformation, and movement of intercrystalline boundaries during crystal lattice transformations [5].

The orientation of two neighboring crystals (local texture) determines the structure of a boundary between them and its mobility [6]. Therefore, the local texture determines the possibility and directionality of a process of both structural (recrystallization) and phase transformations. Description of these processes in "the language of crystallography" at a minimum signifies an understanding of atomic mechanisms of transformations, and makes it possible to control these mechanisms to the maximum due to intentional actions.

Use of high-strength steels capable of operating under complex climatic conditions is one of the most promising ways of improving the economic efficiency of main pipelines as a result of increasing the operating pressure within them [7, 8]. An advantage of using high-strength pipes is a reduction in their metal content [7 – 9]. A marked improvement in low-alloy pipe steels of strength classes X52 – X65 and X70 – X80 and higher towards X1000 was made it possible in the middle of the 1970s in view of development and introduction into industrial production of thermomechanical controlled processing (TMCP) combining controlled rolling in the austenitic region and subsequent accelerated controlled cooling into a process that implements $\gamma \rightarrow \alpha$-shear transformation [7, 10, 11]. Achievement of high-strength classes is a consequence of a change-over from ferrite-pearlite structures to products of shear transformations, i.e., predominantly bainite, whose stable preparation provides control of supercooled austenite stability due to alloying and use of controlled accelerated cooling [12 – 15].

It has been shown in [15, 16] that in spite of the multivariant nature of orientations of the BCC-lattice arising during shear transformation of austenite, strips (sheets) subjected to TMCP have presence of an expressed crystallographic texture. It has been shown in [15, 17] that a marked role in processes of pipe steel failure for main pipelines is

[1] G. I. Nosov Magnitogorsk State Technical University, Magnitogorsk, Russia (e-mail: psipsi@mail.ru).
[2] Magnitogorsk Metallurgical Combine, Magnitogorsk, Russia.
[3] ITTs Ausferr, Magnitogorsk, Russia.
[4] B. N. El'tsin Ural Federal University, Ekaterinburg, Russia (e-mail: m.l.lobanov@urfu.ru).

**TABLE 1.** Microstructure and Texture Parameters Through Steel 06G2MB Thickness after TCMP

| Area nominal No. | $R_h$, mm | $R_h$, proportion of $h$ | Amount of tempered martensite, % | Bainite properties | | |
|---|---|---|---|---|---|---|
| | | | | $D_{av}$, μm | $X_{av}/D_{av}$ | Texture main components |
| *1* | 1.5 | 0.06 | 6.8 ± 0.6 | 1.2 ± 0.1 | 2.06 | Strong: two of {110}⟨112⟩; weak: two of {110}⟨110⟩ |
| *2* | 2.6 | 0.13 | 6.1 ± 0.5 | 1.4 ± 0.1 | 2.12 | Strong: two of {112}⟨110⟩; weak: two of {110}⟨112⟩ |
| *3* | 5.7 | 0.22 | 6.0 ± 0.5 | 1.6 ± 0.1 | 2.35 | Strong: (001)[110]; weak: two of {110}⟨112⟩ |
| *4* | 6.5 | 0.25 | 7.6 ± 0.6 | 1.5 ± 0.1 | 2.23 | Strong: two of {112}⟨110⟩; weak: two of {111}⟨112⟩ |
| *5* | 9.9 | 0.38 | 7.5 ± 0.6 | 1.3 ± 0.1 | 2.34 | Strong: two of {112}–{113}⟨110⟩; weak: two of {111}⟨112⟩; two of {111}⟨110⟩; one of (001)[110] |
| *6* | 10.8 | 0.42 | 9.4 ± 0.7 | 1.4 ± 0.1 | 2.14 | ″ |
| *7* | 12.7 | 0.49 | 9.3 ± 0.7 | 1.4 ± 0.1 | 2.13 | ″ |

played not by the integral texture of a component, but one of its weak components, i.e., (001)[110]. In order to develop cracks presence of quite extensive regions with the corresponding orientation over its length is important, exceeding the critical crack size.

The aim of the present work is revelation of features of structural and textural condition formation in industrial strips of low-carbon low-alloy steel prepared using TMCP.

## METHODS OF STUDY

The specimens studied were cut from the central region of industrial strip of low-carbon low-alloy pipe steel type 06G2MB (wt.%: about 0.05 C, ≤ 2.0 Mn, about 0.2 Mo, about 0.05 Nb, balance Fe and unavoidable impurities), intended for manufacturing pipes of considerable diameter of strength classes K60, K65 (X70, X80). The temperature for the end of isothermal hot rolling during TMCP was close to the $Ac_3$ temperature for this steel and was about 830°C.

Specimens were prepared for total thickness $h$ of strip (25 mm) and had the following mechanical properties: $\sigma_y$ = 550 ± 10 MPa, $\sigma_r$ = 680 ± 10 MPa, $\delta_5$ = 23 ± 2%; $\delta_r$ = 10.5 ± 0.5%; $KCU^{-60}$ = 3.70 ± 0.3 mJ/m$^2$; $KCU^{-40}$ = 3.84 ± 0.06 mJ/m$^2$.

In specimens over the whole thickness $h$ metallographic microsections were prepared in plane RD-TD (where RD is rolling direction during TMCP, TD is the transverse direction to RD), and at differences distances $R_h$ from the strip surface (along the normal direction to the rolling plane, ND) the microstructure and texture were tested (see Table 1).

Electron microscope study of the structure was performed in a Tescan Mira 3 with an auto-emission cathode with an accelerating voltage of 20 kV. In order to determine the orientation of individual grains and to analyze the local texture an Oxford Instrument EBSD HKL Inca analysis system was used. Test areas had a size of 1000 × 1000 μm, and the scanning step was 100 nm. The error for determining crystal lattice orientation was $< \pm 1°$ (on average ± 0.6°). Low-angle boundaries between local volumes were plotted on orientation maps with misorientations from 2 to 15°, and with misorientations not less than 15° high-angle boundaries were provided.

The high accuracy of orientation identification and correspondingly local misorientations during performance of BSD analysis (> 95% recognition for all test regions) made it possible to use the Oxford Instrument software for determining parameters of the specimen microstructure: average crystallite size ($X_{av}/D_{av}$) (see Table 1). $D_{av}$ was determined as the diameter of a circle of equivalent crystallite average area. As crystallite an object was adopted bounded on all sides by boundaries with a misorientation angle not less than 15°.

Analysis of special boundaries between individual grains was accomplished by plotting them on orientation maps taking account provision in the software of the Brandon standard criterion $\pm\Delta\Theta$. For each value boundary is comprised a specific value: $\Delta\Theta = 15°/(\Sigma n)^{1/2}$, where $\Sigma n$ is number of coincident angles with superimposition of three-dimensional crystal lattices. A study of the texture was conducted using construction orientation distribution functions (ODF). During analysis of orientations a coordinate system was adopted whose axes were connected with the hot-rolling direction during TMCP ($X \parallel$ RD), normal to its plane ($Y \parallel$ RD) and with the transverse direction ($Z \parallel$ TD), which coincides with the axis of rolls so that all directions for a regular trio of vectors.

## RESULTS AND DISCUSSION

In both surface and central layers of specimens a record was made of the extent of regions with almost parallel

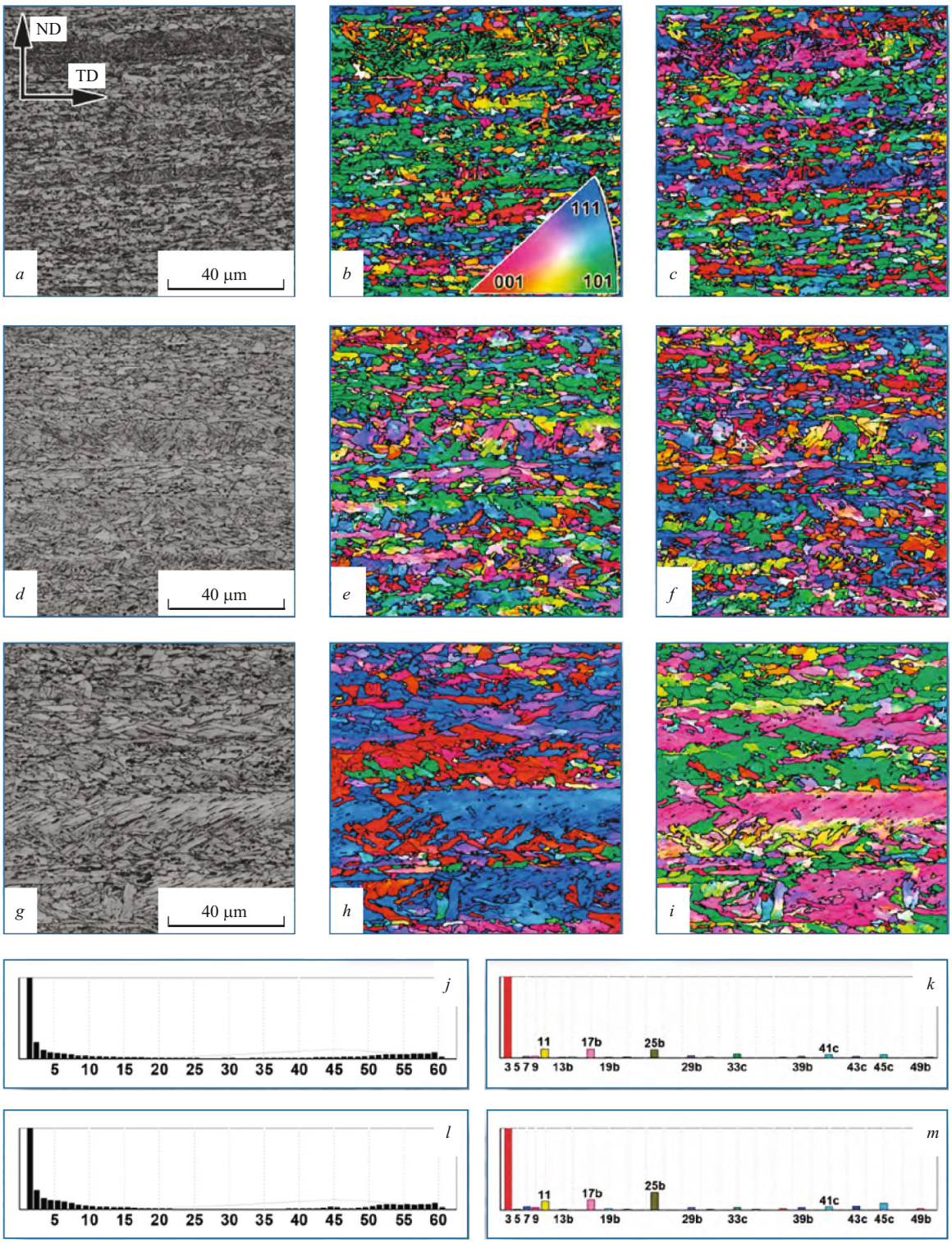


**Fig. 1.** Steel 06G2MB microstructure after TMCP at a different distance from strip surface; *a* – *c*, *j*, *k* ) 1.5 mm; *d* – *f*, *l*, *m* ) 10.8 mm; *a*, *d*, *g* ) orientation contrast in back-scattered electrons; *b*, *e*, *h* ) orientation maps (EBSD) in color with ND Y (in Fig. 1*b* a stereographic triangle is given with color differentiation of crystallographic directions); *c*, *f*, *i* ) orientation maps (EBSD) in color with TD Y; *j*, *l* ) intercrystalline boundary distribution with respect to misorientation angle; *k*, *m* ) RSU boundary spectra.

boundaries extended in the RD with thickness of 5 – 30 μm (Fig. 1*a* – *e*). It is apparent that these regions corresponded to deformation as a result of controlled rolling of austenite grains.

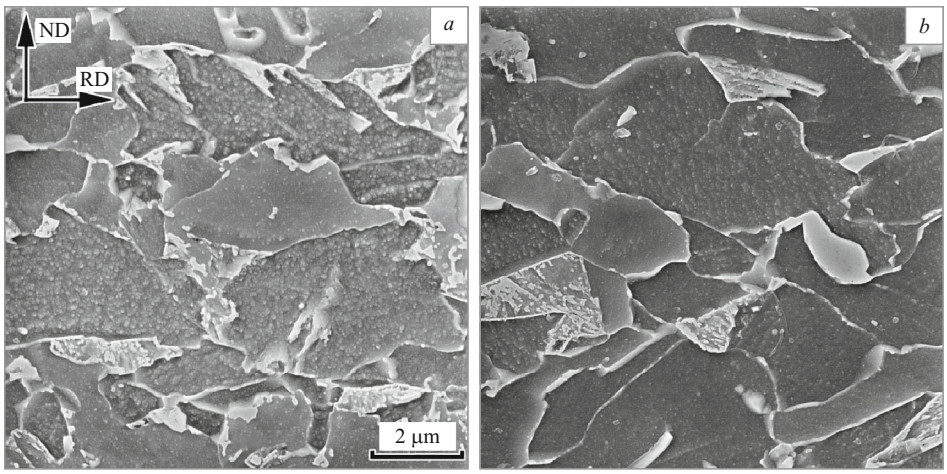


**Fig. 2.** Steel 06G2MB microstructure in reflected electrons at different distances from strip surface: *a*) 1.5 mm; *b* ) 12.6 mm.

Within specimen surface layers ($R_h \le 2$ mm) alternation was observed for extended regions corresponding to deformed austenite grains with two different structures (Fig. 1*a* – c). A bundle structure typical for martensite was rarely recorded, consisting of fine laths. The main proportion was occupied by a region consisting of coarser individual (not bindle) crystallites characterized by extension along the RD of irregular forms having a size of up to 30 μm with $D_{av}$ ~ 1.2 μm (see Table 1).

At a distance from the surface $R_h \ge 3$ mm within the structure martensite bundles almost disappear. This structure is represented by non-equiaxed crystals somewhat extended along the RD, and with fine "shaded" inclusions at their boundaries (Fig. 1*d* ). At high magnification (Fig. 2) it is seen that these inclusions are not precipitates, but are characterized by presence of an inherent structure apparently consisting of several phases.

The average sizes of crystallites of the main structural component increased somewhat to $D_{av}$ ~ 1.6 μm at distance from the surface of about 6 mm. With a subsequent increase in $R_h$ the average diameter of crystallites varied insignificantly (see Table 1). It is important to note that within central areas of a specimen ($0.4h \le R_h \le 0.5h$) within the structure it also possible to observe comparatively large uniform areas extended along the RD ($D_X > 100$ μm) corresponding to deformed austenite grains, without high-angle intercrystalline boundaries (Fig. 1*g* – *i* ). Apparently it is possible to confirm that in this case $\gamma \rightarrow \alpha$-transformation proceeds with replacement of one deformed austenite grain by one ferritic (bainitic) grain, or by a collection of bainitic grains having almost the same crystallographic orientation (Fig. 1*h* and *i* ).

From the surface towards the center there is an increase in both the volume fraction and size of "dark" inclusions (Fig. 1*a*, *d*, and *g* ). Results of orientation microscopy make it possible to confirm that inclusions are tempered martensite bundles with carbide precipitates between laths. These areas correspond to austenite enriched with carbon, whose decomposition during cooling is subsequently realized. Differences in the microstructure of surface and central layers are connected with a reduction in cooling rate during TMCP from the surface towards the center of strip.

For the whole specimen cross section spectra of intercrystalline boundaries corresponded to the structure obtained as a result of shear phase transformations (Fig. 1*j* – *m* ) in accordance with orientation relationships (OR), intermediate between Kurdyumov–Zaks (K-Z) and Nishiyami–Wasserman (N-W) OR. The main proportion of high-angle boundaries is concentrated at misorientation angles from 49 to 60° (see Fig. 1*j* and *l* ). With the spectrum of special boundaries RSA-boundaries Σ3, Σ11, Σ25b, Σ33c, Σ41c (Fig. 1*k* and *m* ) were predominantly recorded. A small number of RSA boundaries was also observed Σ7, Σ9, Σ17b, Σ29b, Σ31b, Σ39b, Σ43c, and Σ45c. According to analysis conducted in [19] occurrence of a considerable number of them is connected with implementation of relaxation processes (polygonization and the start of primary recrystallization) in a BCC-lattice. It is apparent that all structures recorded through the strip thickness after TMCP should be considered as predominantly bainitic with inclusions of tempered martensite.

The texture of a central layer revealed by the EBSD method, i.e., at a distance from the surface of $0.3h - 0.5h$ (Fig. 3; Table 1) consists of a discrete collection of components: two strongly expressed orientations of {112}⟨110⟩, dispersed through {113}⟨110⟩; comparatively weak, i.e., two of {111}⟨110⟩, two of {111}⟨112⟩ and (001)[110]. This coincides with the TMCP texture provided in [15, 16, 20, 21]. The surface layer texture differs considerably from that of the central layer. It consists of a component corresponding to the central area turned by 90° around the RD. The ratio of central and surface textural components is typical with defor-

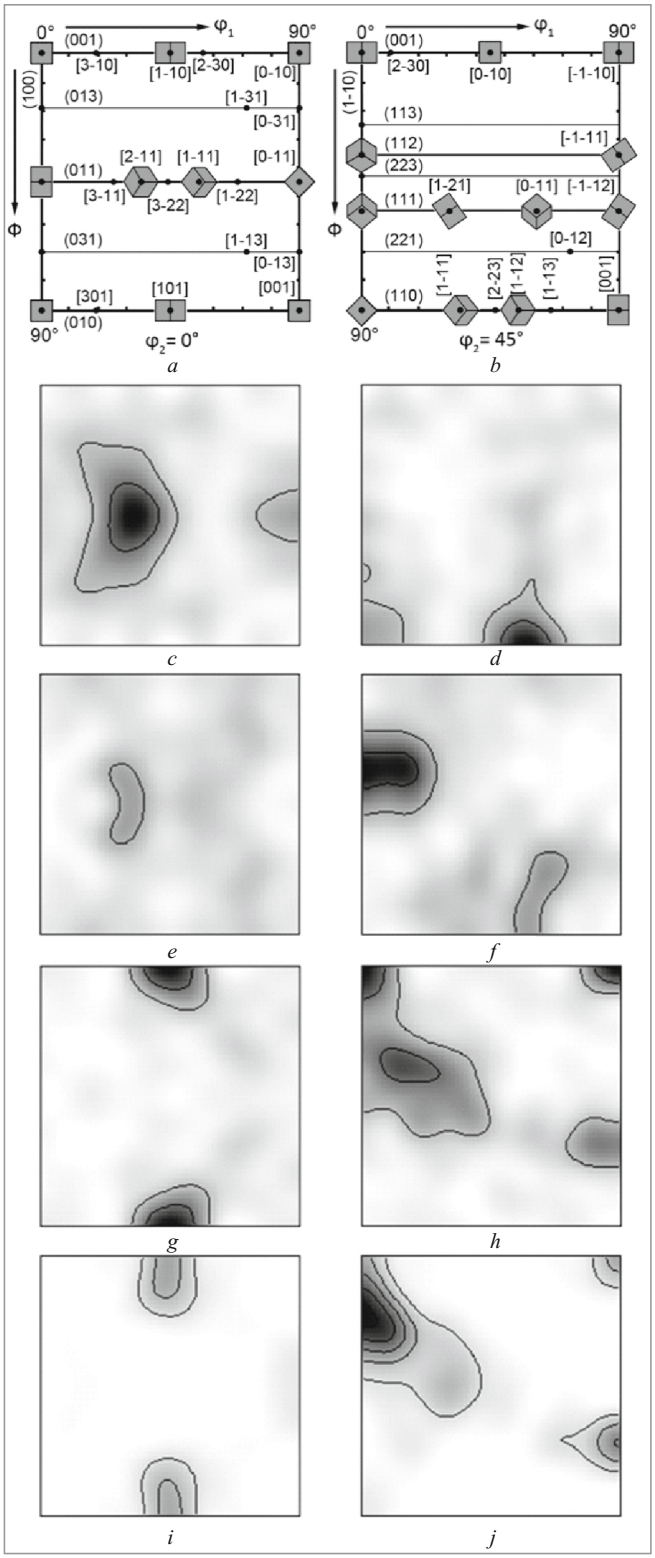


**Fig. 3.** Steel 06G2MB texture after TMCP in the form of ODF (EBSD). Euler angle spatial sections are provided with $\varphi_2 = 0°$, $\varphi_2 = 45°$: *a*, *b* ) standard networks for ODF sections with $\varphi_2 = 0°$ and $\varphi_2 = 45°$ respectively with application of ideal orientations in the form of elementary crystallographic cells (form with TD); *c*, *d* ) ODF of region at distance from surface $R_{h=}$ 1.5 mm; *e*, *f* ) $R_h$ = 5.7 mm; *g* ) $R_h$ = 9.9 mm; *h*, *i* ) $R_h$ = 12.7 mm.

mation of metal hot rolled texture with cubic lattices [22, 23]. This ratio is due to implementation in the surface and central areas of material rolled at high temperature of different stressed states as a result of the considerable magnitude of friction between rolls and strip. The texture of layers at a distance of $0.2h - 0.3h$ from surface contains components typical both for the surface and within central layers (see Table 1; Fig. 3*c* ).

Formation of a TMCP texture in the form of a comparatively small selection of components: 3 – 7 (see Table 1) with multi-variance of crystallographic orientations arising in steels with shear phase transformation; $n \times m > 100$ {where $n$ is the number of stable deformation orientations of the BCC-lattice (7 – 9) [24]; $m$ is the number of orientations of BCC-lattice formed in accordance with K-Z OS (24 orientations) or N-W OS (12 orientations) [24, 25]}, suggests presence within the structure of some elements limiting the number of possible orientations of α′-phase, According to data in [16, 18] these elements are special boundaries formed during hot rolling close to boundaries of RSC ∑3 and probably ∑11 between deformed austenite grains.

Use of special boundaries as “carriers” of structural-textural inheritance is entirely correct. Only for similar boundaries is it possible to describe their movement at the level of slip and dislocation sliding. Also presence and movement of special boundaries quite simply explains formation and development of local textures in polycrystalline materials during structural transformations [19, 26 – 28]. It should be emphasized that in a BCC-lattice, according to both theoretical calculations ad experimental observations, special boundaries ∑3 and ∑11 exhibit minimum surface energy [5], they may be substrates for generation of new phases or a new grain. It should also be noted that special boundaries close to the phase transition temperature may a source of transformation dislocations.

## CONCLUSIONS

It has been demonstrated that the fineness of martensite-bainite structures in the surface and central areas of strip of low-carbon low-alloy steel is determined by the cooling rate for steel layers during TMCP. Formation of a TMCP structure in the form of a comparatively small collection of components (3 – 7) with multivariance of crystallographic orientations arising in steel with shear phase transformations in accordance with Kurdyumov–Zaks OR or Nishiyami–Wassereman OR (> 100) suggests presence within the structure of elements limiting the number of possible orientations of α′-phase. These elements are formed during hot rolling of special boundaries close to the RSA boundaries ∑3 and ∑11 between deformed austenite grains.

*The authors are grateful for the support of leading RF universities with the aim of increasing their competitiveness*

*of No. 211 of the RF Government No. 02.A03.21.0006. The authors thank PASO MMK for support and cooperation in organizing research. The work was conducted with support of a stipend from the President of the Russian Federation for project SP-259.2018.1.*

## REFERENCES


1. W. B. Hutchinson, " Practical aspects of texture control in low carbon steels," *Mater. Sci. Forum*, **157 – 162**, 1917 – 1928 (1994).
2. D. Lindell, "Texture evolution of warm-rolled and annealed 304L and 316L austenitic stainless steels," *IOP Conf. Ser.: Mater. Sci. Eng.*, **82**, Art. No. 012101 (2015).
3. A. V. Druker, C. Sobrero, V. Fuster, et al., "Is it possible to use rolling methods to improve textures on Fe – Mn – Si shape memory alloys?" *Adv. Eng. Mater.*, **20**(4), Art. No. 1700062 (2017).
4. A. I. Rudskoy, A. A., Kononov, S. Yu., Kondrat'ev, and M. A. Matveev, "Texture formation in hot rolling of electrical anisotropic steel," *Met. Sci. Heat Treat.*, **60**(11 – 12), 689 – 694 (2019).
5. F. J. Humphreys and M. Hatherly, *Recrystallization and Related Annealing Phenomena*, ELSEVIER Ltd., Oxford (2004).
6. O. A. Kaibyshev and R. Z. Valiev, *Grain Boundaries and Metal Properties* [in Russian], Metallurgiya, Moscow (1987).
7. K. Khulka, P. Peters, and F. Khaisterkamp, "Trends in the development of steels for large diameter pipes," *Stal'*, No. 10, 62 – 67 (1997).
8. E. Shigeru and N. Naoki, "Development of thermo-mechanical control process (TMCP) and high performance steel in JFE steel," *JFE Tech. Report*, No. 20, 1 – 7 (2015).
9. Yu. D. Morozov, S. Yu. Nastich, M. Yu. Matrosov, and O. N. Chevskaya, "Obtaining high-quality properties of rolled material for large-diameter pipes based on formation of ferrite-bainite microstructure," *Metallurgist*, **52**, 21 – 28 (2008).
10. S. Y. Nastich, Y. D. Morozov, V. L. Kornilov, et al., "New steels for pipelines of strength classes K54 – K60 (X70): Production experience at OAO MMK," *Steel in Translation*, **39**, 431 – 436 (2009).
11. H. K. Sung, S. Y. Shin, B. Hwang, et al., "Effects of carbon equivalent and cooling rate on tensile and Charpy impact properties of high-strength bainitic steels," *Mater. Sci. Eng. A*, **530**, 530 – 538 (2011).
12. Z. J. Xie, X. P. Ma, C. J. Shang, et al., "Nano-sized precipitation and properties of a low carbon niobium micro-alloyed bainitic steel," *Mater. Sci. Eng. A*, **641**, 37 – 44 (2015).
13. E. A. Goli-Oglu, L. I. Éfron, and Yu. D. Morozov, "Effect of deformation regime in main stages of controlled rolling on pipe steel microstructure," *Met. Sci. Heat Treat.*, **55**(5 – 6), 294 – 297 (2013).
14. M. L. Lobanov, S. V. Danilov, V. I. Pastukhov, et al., "Effect of cooling rate on the structure of low-carbon steel after controlled thermomechanical treatment," *MiTOM*, No. 1, 31 – 37 (2019).
15. I. Y. Pyshmintsev, A. O. Struin, A. M. Gervasyev, et al., "Effect of bainite crystallographic texture on failure of pipe steel sheets made by controlled thermomechanical treatment," *Metallurgist*, **60**, 405 – 412 (2016).
16. M. L. Lobanov, M. D. Borodina, S. V. Danilov, et al., "Texture inheritance on phase transition in low-carbon, low-alloy pipe steel after thermomechanical controlled processing," *Steel in Translation*, **47**, 710 – 716 (2017).
17. M.-C. Zhao, K. Yang, and Y. Shan, "The effects of thermo-mechanical control process on microstructures and mechanical properties of a commercial pipeline steel," *Mater. Sci. Eng. A*, **335**, 14 – 20 (2002).
18. M. L. Lobanov, G. M. Rusakov, A. A. Redikul'tsev, et al., "Investigation of special misorientations in lath martensite of low-carbon steel using the method of orientation microscopy," *Phys. Met. Metallogr.*, **117**, 254 – 259 (2016).
19. G. M. Rusakov, M. L. Lobanov, A. A. Redikul'tsev and A. S. Belyaevskikh, "Special misorientations and textural heredity in the commercial alloy Fe – 3% Si," *Phys. Met. Metallogr.*, **115**, 775 – 785. (2014).
20. B. Hutchinson, L. Ryde, E. Lindh, and K. Tagashira, "Texture in hot rolled austenite and resulting transformation products," *Mater. Sci. Eng. A*, **257**, 9 – 17 (1998).
21. X. Yang, Y. Xu, X. Tan, and D. Wu, "Influences of crystallography and delamination on anisotropy of Charpy impact toughness in API X100 pipeline steel," *Mater. Sci. Eng. A*, **607**, 53 – 62 (2014).
22. M. L. Lobanov, A. A. Redikul'tsev, G. M. Rusakov, and S. V. Danilov, "Interrelation between the orientations of deformation and recrystallization in hot rolling of anisotropic electrical steel," *Met. Sci. Heat Treat.*, **57**(5 – 6), 492 – 497 (2015).
23. M. L. Lobanov, Y. N. Loginov, S. V. Danilov, et al. "Effect of hot rolling rate on the structure and texture condition of plates of the Al – Si – Mg alloy system," *Met. Sci. Heat Treat.*, **60**(5 – 6), 329 – 336 (2018).
24. M. Hölscher, D. Raabe, and K. Lücke, "Relationship between rolling textures and shear textures in F.C.C. and B.C.C. metals," *Acta Metall. Mater.*, **42**, 879 – 886 (1994).
25. W. Gong, Y. Tomota, A. M. Paradowska, et al., "Effects of ausforming temperature on bainite transformation, microstructure and variant selection in nanobainite steel," *Acta Mater.*, **61**, 4142 – 4154 (2013).
26. I. Sabirov, I. de Diego-Calderón, J. M. Molina-Aldareguia, et al., "Microstructural design in quenched and partitioned (Q&P) steels to improve their fracture properties," *Mater. Sci. Eng. A,* **657**, 136 – 146 (2016).
27. M. L. Lobanov, S. V. Danilov, V. I. Pastukhov, et al., "The crystallographic relationship of molybdenum textures after hot rolling and recrystallization," *Mater. Design*, **109**, 251 – 255 (2016).
28. V. A. Nekit, S. I. Platov, I. A. Kurbakov, and A. D. Golev, "Experimental study of forward slip and delays during rolling," *Vestn. Magnit. Gos. Tekhn. Univ. im. G. I. Nosova*, No. 1(49), 52 – 54 (2015).